JOURNAL OF BACTERIOLOGY, Mar. 1993, p. 1814–1822
0021-9193/93/061814-09$02.00/0

Vol. 175, No. 6

Electron Microscopic Analysis and Structural Characterization of Novel NADP(H)-Containing Methanol: *N,N'*-Dimethyl-4-Nitrosoaniline Oxidoreductases from the Gram-Positive Methylotrophic Bacteria *Amycolatopsis methanolica* and *Mycobacterium gastri* MB19

LEONID V. BYSTRYKH,[1] JANET VONCK,[2]† ERNST F. J. VAN BRUGGEN,[2] JOZEF VAN BEEUMEN,[3] BART SAMYN,[3] NATALYA I. GOVORUKHINA,[1] NICO ARFMAN,[1] JOHANNIS A. DUINE,[4] AND LUBBERT DIJKHUIZEN[1]*

Department of Microbiology, University of Groningen, Kerklaan 30, NL-9751 NN Haren,[1] BIOSON Research Institute, University of Groningen, Nijenborgh 4, NL-9747 AG Groningen,[2] and Department of Microbiology and Enzymology, Delft University of Technology, Julianalaan 67, NL-2608 BC Delft,[4] The Netherlands, and Laboratory of Microbiology and Microbial Genetics, University of Gent, B-9000 Ghent, Belgium[3]

Received 10 August 1992/Accepted 14 January 1993

The quaternary protein structure of two methanol:*N,N'*-dimethyl-4-nitrosoaniline (NDMA) oxidoreductases purified from *Amycolatopsis methanolica* and *Mycobacterium gastri* MB19 was analyzed by electron microscopy and image processing. The enzymes are decameric proteins (displaying fivefold symmetry) with estimated molecular masses of 490 to 500 kDa based on their subunit molecular masses of 49 to 50 kDa. Both methanol:NDMA oxidoreductases possess a tightly but noncovalently bound NADP(H) cofactor at an NADPH-to-subunit molar ratio of 0.7. These cofactors are redox active toward alcohol and aldehyde substrates. Both enzymes contain significant amounts of Zn^{2+} and Mg^{2+} ions. The primary amino acid sequences of the *A. methanolica* and *M. gastri* MB19 methanol:NDMA oxidoreductases share a high degree of identity, as indicated by N-terminal sequence analysis (63% identity among the first 27 N-terminal amino acids), internal peptide sequence analysis, and overall amino acid composition. The amino acid sequence analysis also revealed significant similarity to a decameric methanol dehydrogenase of *Bacillus methanolicus* C1.

Only limited information about the identity and properties of methanol-oxidizing enzymes in gram-positive methylotrophic bacteria is currently available. Thermotolerant *Bacillus* strains have been previously shown (3, 5) to employ an unusual NAD-dependent methanol dehydrogenase (MDH) (EC 1.1.1.1). This decameric enzyme has been shown to contain a tightly associated (noncovalent) NAD(H) molecule in each subunit, as well as zinc and magnesium ions. The activity of this enzyme is strongly stimulated by a specific activator protein (4, 24). The MDH enzyme does not share homology with either long-chain or short-chain alcohol dehydrogenases (16) but appears to belong to a recently established third family of alcohol dehydrogenases (10).

The situation with the gram-positive methylotrophic bacteria *Amycolatopsis methanolica* and *Mycobacterium gastri* MB19 is less clear (6, 9). These organisms possess enzymes catalyzing the oxidation of methanol with the concomitant reduction of the artificial electron acceptor *N,N'*-dimethyl-4-nitrosoaniline and dismutate formaldehyde, producing methanol and formate. No alcohol-dependent reduction of coenzyme NAD(P) by these enzymes could be detected, and they are referred to as methanol:*N,N'*-dimethyl-4-nitrosoaniline oxidoreductases (MNOs). Purification and characterization of the MNO enzymes present in methanol-grown cells of *A. methanolica* and *M. gastri* revealed that they are homopolymers of 49- to 50-kDa subunits; gel filtration chromatography indicated a native M_r of approximately 255,000 to 268,000 (6). Here, we present the quaternary structure of the *A. methanolica* and *M. gastri* MNOs as analyzed by electron microscopy and image processing. In addition, their cofactor and metal compositions, as well as the amino acid sequences of the N termini and several internal peptide fragments, are compared with those of various alcohol dehydrogenases.

MATERIALS AND METHODS

Growth conditions and enzyme purification. The growth of *A. methanolica* and *M. gastri* MB19 and the purification of the MNO enzymes from these organisms were performed as described by Bystrykh et al. (6).

Electron microscopy. Specimens for electron microscopy were prepared by applying a drop of MNO, at a concentration of 0.5 mg/ml, to grids covered with a carbon-coated Formvar film which had been treated by a glow discharge in pentylamine immediately before being used. The specimens were blotted with filter paper and negatively stained with a solution of 2% (wt/vol) sodium silicotungstate or 1% (wt/vol) uranyl acetate.

Electron microscopy was performed with a Philips CM12 or a JEOL JEM 1200 EX, both operating at 80 kV. With both microscopes, a low-dose system was used for focussing on an area adjacent to the area to be imaged, in order to avoid

* Corresponding author.
† Present address: Division of Cell and Molecular Biology, Lawrence Berkeley Laboratory, University of California, Berkeley, CA 94720.

unnecessary irradiation. Images were recorded on Agfa Scientia 23D56 film at an electron optical magnification of 60,000×.

Image processing. Electron micrographs checked by optical diffraction for proper focussing and lack of drift and astigmatism were digitized on a Joyce-Loebl Scandig 3 rotating drum densitometer with a step size of 25 μm, which corresponds to 0.4 nm at the specimen level.

Image analysis was carried out with a Convex C1-XP minisupercomputer with the Imagic software system (22), as described earlier (24). Different classes present in the data set were identified by correspondence analysis (11, 21) followed by hierarchical ascendant classification (20, 23). Correspondence analysis groups the images in a multidimensional space in such a way that their proximity is a measure of their similarity. The multidimensional cloud is visualized by projecting along the directions of largest extent, i.e., the largest intermolecular differences. Hierarchical ascendant classification divides the data set into groups with the highest inter-class and the lowest intraclass variances.

Computer model building. Model building was done with a Commodore Amiga 2000 with the Sculpt-Animate-3D program (Byte by Byte Corporation, Austin, Tex.).

Spectrophotometry. UV-visible (UV-VIS) absorption spectra (250- to 400-nm region) were measured with an AMINCO DW-2000 double-beam recording spectrophotometer. About 0.4 mg of MNO was incubated in 1 ml of a 0.1 M potassium phosphate buffer (pH 6.3) in a 10-mm-wide quartz cuvette. Methanol (25 mM), formaldehyde (1 mM), and acetaldehyde (9 mM) were added as indicated.

Fluorescence spectra were recorded at 30°C with a Perkin-Elmer Luminescence Spectrometer, type LS 50. Measurements were performed with a quartz cuvette (10 mm wide) and 3 ml of 0.1 M Tris-HCl buffer, pH 8.0. Fluorescence excitation spectra of the purified MNO from *A. methanolica* were scanned in the range of 260 to 400 nm (band width, 15 nm) at a fixed emission wavelength of 430 nm. Fluorescence emission spectra were scanned in the range of 350 to 550 nm (band width, 15 nm) at a fixed excitation wavelength of 340 nm. To check the redox activity of the MNO-bound pyridine nucleotide, the following substrates were added: methanol, 25 mM; formaldehyde, 1 mM; and acetaldehyde, 90 mM. A solution of commercial NADPH (30 nmol; Boehringer, Inc.) in the same buffer served as a standard. Spectra were corrected against Tris-HCl buffer (as indicated above) with FL Data Manager (Perkin-Elmer) installed on an IBM-type personal computer.

Analysis of the cofactor. The cofactor present in the purified MNO preparations from *A. methanolica* and *M. gastri* was extracted with a 6 M urea solution prepared in 0.1 M Tris-HCl buffer, pH 8.5 (1 min, 60°C). Samples were analyzed by ion-exchange chromatography with a Mono Q HR 5/5 column (Pharmacia), equilibrated with 10 mM Tris-HCl buffer (pH 8.5) containing 6 M urea, at a flow rate of 0.5 ml/min. Elution was performed with a 0 to 1 M KCl gradient (15 min) in the same buffer with UV detection at 340 nm. Samples of commercial NADH and NADPH (2 to 5 nmol; Boehringer, Inc.) served as standards.

The cofactor was also analyzed with a high-performance liquid chromatography (HPLC) μBondapak C18 (1.5 by 30 cm) reversed-phase column (Waters). In this case, samples were denatured with trichloroacetic acid at a final concentration of 5%. The denatured protein was spun down by centrifugation in a minicentrifuge. Supernatants containing the extracted chromophore were applied to the column. The column was equilibrated with 0.13 M ammonium acetate buffer, pH 6.2, containing methanol (14 ml/liter) and acetonitrile (10 ml/liter of buffer), and a flow rate of 0.4 ml/min was used. The eluent was analyzed by monitoring the A_{260}. NAD (50 μl of a 1 μM stock solution) served as a standard. These conditions are suitable for the detection of NAD and NADP, but not that of their reduced forms.

The presence of NADPH was also checked via a biological assay. The assay mixture (1 ml) contained 0.1 M Tris-HCl buffer, 0.5 mM 3-(4,5-dimethylthiazol-2-yl)-2,5-diphenyltetrazolium bromide (MTT) (Sigma Chemical Co.), 0.05 mM phenazine methosulfate, glucose-6-phosphate dehydrogenase (NADP specific; 0.1 U), and samples of fast-protein liquid chromatography (FPLC) Mono Q column fractions. Phenazine methosulfate and MTT were added to oxidize the reduced pyridine nucleotides present. After stabilization of the A_{550}, 1 mM glucose-6-phosphate was added to start the reaction.

Amino acid sequence analysis. The N-terminal amino acid sequences of the purified MNO enzymes were determined by automated Edman degradation (15) with a 477A pulsed-liquid sequenator (Applied Biosystems). The phenylthiohydantoin amino acid derivatives were identified by an on-line phenylthiohydantoin analyzer, model 120A (Applied Biosystems), as described by the manufacturer. The runs on the native MNO enzymes were carried out in duplicate, starting with 1 and 2 nm in each case. Amino acid compositional analysis was carried out with a 420A Derivatiser with on-line detection of the phenylthiocarbamyl amino acid derivatives on a 130A Separation System (Applied Biosystems). Hydrolysis of the samples was performed at 106°C for 24 h with 6 N HCl in the gas phase with a Waters reaction vial.

Peptides of each MNO protein were obtained by digesting 20 nm of protein with Lys-C endoproteinase (Wako, Osaka, Japan) at an enzyme/substrate ratio of 1/40 for 2 h at 37°C and in 0.1 M ammonium bicarbonate. The soluble peptides obtained after acidification of the digest mixtures to pH 2 were separated by reversed-phase HPLC with a 5-μm Superpac cartridge PEP-S column (4 by 250 mm) (LKB, Uppsala, Sweden). Gradient elution was performed at 1 ml/min with 0.1% trifluoroacetic acid in water as solvent A and 70% acetonitrile containing 0.1% trifluoroacetic acid in water as solvent B.

Metal analyses. The metal composition of the MNO enzymes from *A. methanolica* and *M. gastri* was determined with a Perkin-Elmer 5100 oven atomic absorption spectrophotometer. The purified protein preparations were dialyzed extensively against 10 mM Tris-HCl buffer, pH 7.0, containing 1 mM EDTA and subsequently against the same buffer without EDTA. The following elements were analyzed in duplicate: zinc, magnesium, iron, and copper.

Analytical. Pyrroloquinoline quinone was analyzed enzymatically (13). The protein concentration was measured by either a direct spectrophotometric assay (17) or the Bio-Rad protein assay kit (Bradford method) with bovine serum albumin as a standard.

RESULTS

Electron microscopy. Electron micrographs of negatively stained MNOs from *A. methanolica* and *M. gastri* (Fig. 1) reveal very similar structures for both proteins. Fivefold symmetrical projections about 15 nm in diameter, as well as narrower, more rectangular views, can be recognized by eye. In addition, projections of intermediate widths are visible. There is also some smaller material, especially in the

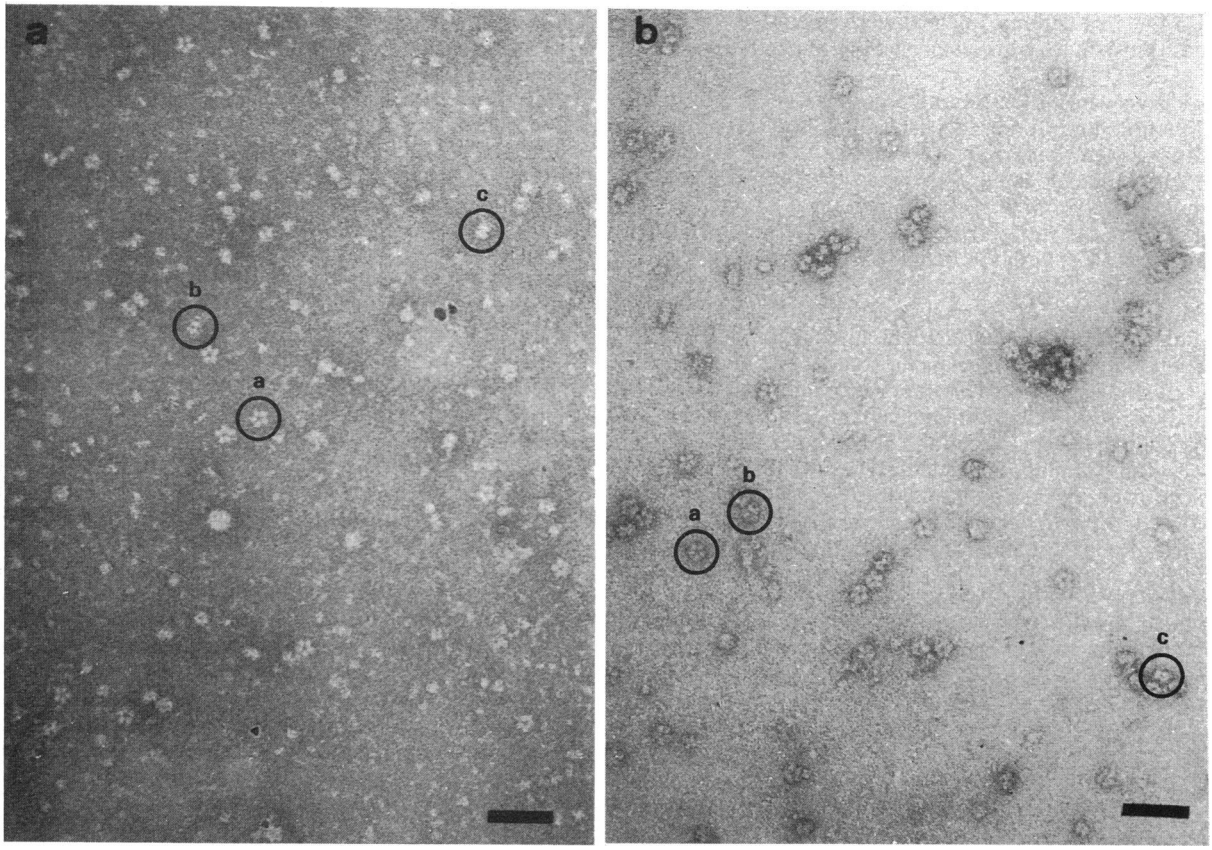

FIG. 1. Electron micrographs of MNOs from *A. methanolica*, negatively stained with 2% sodium silicotungstate (a), and *M. gastri* MB19, negatively stained with 1% uranyl acetate (b). Bar, 50 nm. Recurring projections have been encircled. a, top view; b, broad side view; c, narrow side view.

A. methanolica preparation (Fig. 1a), which is most likely degradation products of the proteins.

It is clear that the MNO proteins of both *A. methanolica* and *M. gastri* have a striking structural resemblance to the previously described decameric MDH protein of *Bacillus methanolicus* C1 (3, 24). Thus, the MNO proteins consist of 10 identical subunits, and on the basis of their subunit molecular masses of 50 and 49 kDa, (6), their deduced native molecular masses would be 500 and 490 kDa, respectively, which are about twofold higher than the values estimated by gel filtration (6).

The two MNO proteins and the *Bacillus* MDH protein in particular share very similar fivefold symmetrical top views. Another feature of the *Bacillus* MDH protein, a clear subdivision along two perpendicular lines in many side views, however, was never observed in the *A. methanolica* and *M. gastri* MNO preparations. Conversely, the intermediate-width views of the latter two proteins were never found in *Bacillus* MDH.

Image processing. The images of approximately 1,400 MNO molecules from *A. methanolica* were processed by computer in order to get a clearer picture of their differences from the *B. methanolicus* C1 MDH enzyme. The top views, which were very easily distinguishable, were selected separately. All images which did not display fivefold symmetry were treated together, regardless of their widths, because they could not be classified unambiguously by eye.

Alignment of 501 top views and subsequent correspondence analysis yielded a homogeneous set of images which did not show any separate classes. Consequently, the 200 images having the highest correlation with the reference were averaged. The average (Fig. 2a) displays fivefold symmetry, and it is very similar to the *Bacillus* MDH protein (24).

The 875 side views were aligned first to a reference showing a clear intermediate-width view. The resulting average of the 100 images having the highest correlation with the reference is shown in Fig. 2b. Correspondence analysis of the aligned side views clearly indicated the presence of more than one view. By multivariate statistical analysis, the data set was separated into nine classes, which automatically excluded 15% of the images. A classification map, with the corresponding class averages, is shown in Fig. 3. The projection of the data set on the two most important axes has a mushroom-like shape. The stalk of the mushroom contains the images similar to the reference image (classes 4 and 7), whereas the hat consists of other views which did not align properly with the reference. (Averaging these classes gives an image which has certain features in common with the reference, but the individual images can be very dissimilar, and the average need not represent a real structure.)

A new reference image showing a narrower projection was chosen, and alignment was performed as before. This also yielded a good average, shown in Fig. 2c. Correspondence analysis and classification indicated again the presence of two distinct views (not shown).

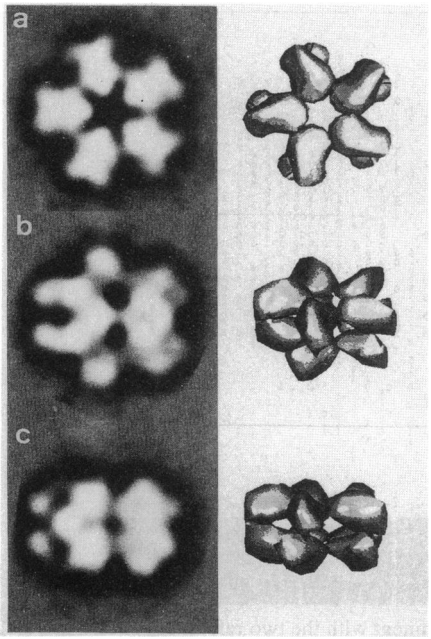

FIG. 2. Averaged projections of *A. methanolica* MNO in several orientations (left) and our interpretations (right). (a) Top view, average of 200 images (no symmetry was imposed); (b) broad side view, average of 100 images; (c) narrow side view, average of 200 images.

Finally, a two-reference alignment was performed with all images by using the final references from the first two alignment cycles. In this procedure, every image is aligned in turn with both references, which yields correlation coefficients between the image and the two references. The translation and rotation determined for the reference with the highest correlation coefficient are applied to the image, which ensures that every image is aligned with the reference it resembles most. Correspondence analysis of the data set after this step shows a clear separation into two classes (Fig. 4). Most of the class averages are similar to one or the other of the references. The smaller class on the left of the map contains the broad projections, and the large class on the right contains the narrow projections.

To determine whether there are any other views present in the data set, independent alignments were performed with several images as the first reference. All alignments converged to either of the two views, indicating that there are no other major classes.

The three MNO projections that were found can be correlated to the model that was proposed for *B. methanolicus* C1 MDH (24). The MNO top view is a view down the fivefold axis, as in the *Bacillus* MDH enzyme. The *A. methanolica* enzyme has a more angular appearance than *Bacillus* MDH, in the center of the molecule as well as on the outer rim, which indicates that the structures are not identical.

The narrow side view (Fig. 2c) is similar to one of the side views in the *Bacillus* enzyme, which was interpreted as a stable position on three subunits with a slight tilt of the molecule. The main differences are a strong stain-excluding patch on the approximate mirror axis of the projection and less clear separation between the two halves (pentamers) of the *A. methanolica* MNO molecule; also, the width/length ratio is slightly higher for *A. methanolica* MNO than for *Bacillus* MDH. This all suggests a slightly higher tilt for *A. methanolica* MNO, indicating a change in shape at the end of the subunits. Such a change can also explain the complete absence in *A. methanolica* (and *M. gastri*) MNO of the orientation most common in the *Bacillus* MDH preparation, a side view possessing twofold symmetry, which was interpreted as a view down a twofold axis with two subunits attached to the support.

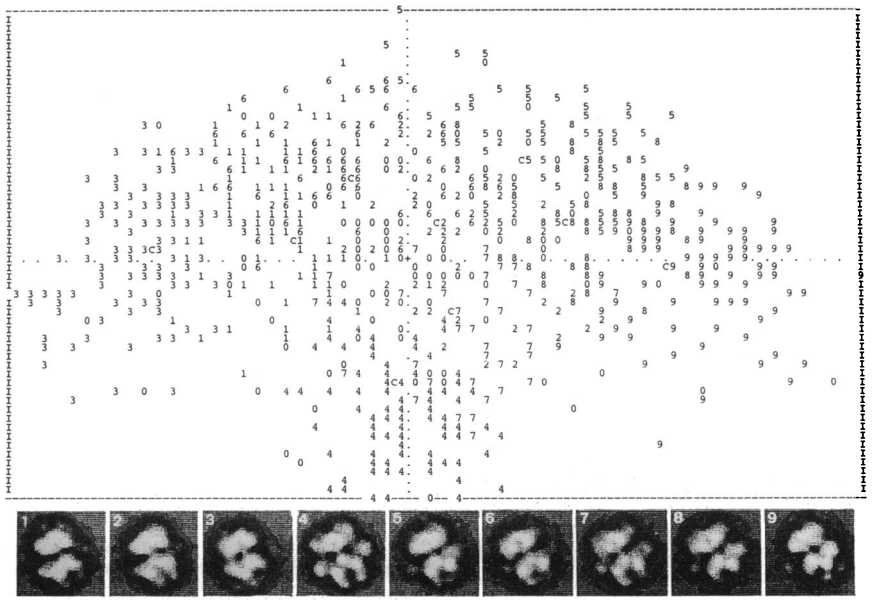

FIG. 3. Classification map of 875 side views of *A. methanolica* MNO after alignment with an image shown in Fig. 2b. The correspondence analysis map of the first two axes is shown. The number of each image has been replaced by the number of the class it was assigned to. Images that were rejected are indicated by zeroes. The class averages of all nine classes are pictured below the map. Classes 1 through 9 contain 108, 74, 107, 102, 66, 74, 45, 65, and 94 members, respectively.

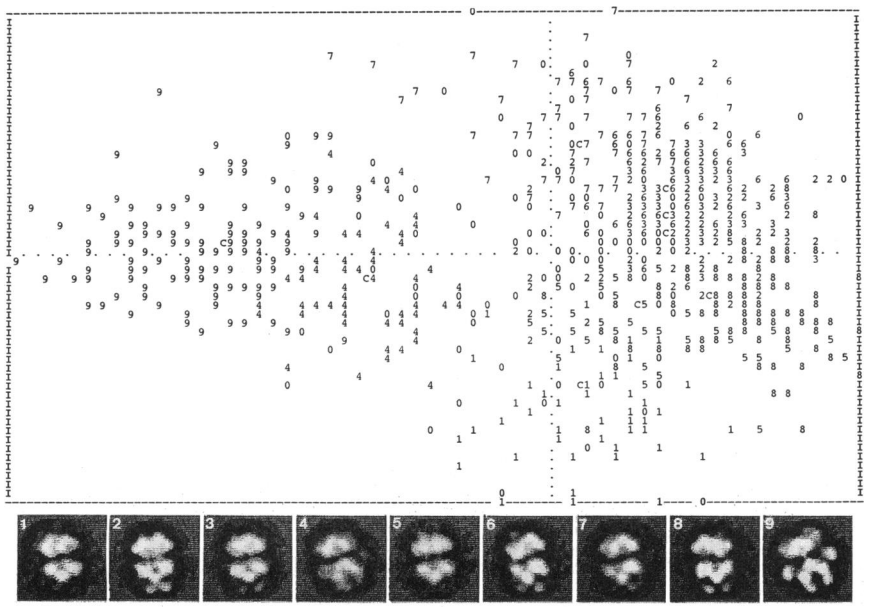

FIG. 4. Classification map of 875 side views of *A. methanolica* MNO after alignment with the two references shown in Fig. 2b and c. The correspondence analysis map of the first versus the second factor is shown. The images are indicated by the number of the class to which they belong. Classes 1 through 9 contain 62, 93, 69, 62, 53, 90, 60, 115, and 132 members, respectively. The class averages are pictured below the map.

The broad side view (Fig. 2b) is very common in the *A. methanolica* (and *M. gastri* [Fig. 1b]) MNO, whereas it was never seen in *Bacillus* MDH. This view can be interpreted as a more highly tilted version of the narrow side view, as shown in Fig. 2c. It is clear that only one subunit makes direct contact with the support film. The rapid density fluctuations seen in the projections are highly reproducible, which means that the broad side view in the *A. methanolica* and *M. gastri* enzymes represents a very stable preferential orientation. This also indicates a substantial difference from *B. methanolicus* C1 MDH, which is located on the end of its subunits.

Amino acid sequence analysis. The high purity of the MNO preparations from *A. methanolica* and *M. gastri* allowed the identification of 47 and 48 N-terminal amino acid residues, 35 and 39 of which could be assigned unambiguously, respectively (Fig. 5). Considerable similarity between the two N-terminal MNO sequences was found: 63% identity in the first 27 amino acid residues, and 81% when conservative substitutions are also considered. No significant N-terminal sequence similarity was apparent with long-chain and short-chain alcohol dehydrogenases (16) and MDH from *B. methanolicus* C1 or other type 3 alcohol dehydrogenases (10, 24). However, alignment of the -Gly-X-Gly- sequence which in type 3 alcohol dehydrogenases occurs around positions 13 to 15 with the same conserved sequence pattern in the two MNO enzymes shows that the evolutionary conserved Leu residue 18 positions downstream from Gly-15 is also present in both MNOs, along with several residues of a conservative nature preceding and following Leu-33 (Fig. 5) (10, 24). This alignment revealed 27 and 30% identity between the first 37 amino acid residues in the *Bacillus* MDH and the *A. methanolica* and *M. gastri* MNO sequences, respectively (54 and 59% similarity, respectively, when conservative substitutions are also considered). A total of 6 residues have been conserved (16% identity) in the three sequences, and 11

```
                                                  1       5         10
MDH                                               M T N F F I P P A S V I G R
AmMNO                 A Q V D E L W K P F P I K E F H P F A R A L L G P
MgMNO                 A I E L N Q I W - D F P I K E F H P F P(R)A L L G V
                        . . . . . *     * * .   . *       .   . . . *

                          15        20        25        30        35
MDH                       G A V K E V G T R L K Q I G A K K A L I V T D
AmMNO                     G A H(D)M I I P(D K L D Q)? F K(K A L V V)T ?
MgMNO                     G A(W D)I(A)G V L A(K)N L G F K(D)T L(L M G)D
                          * *                   .   *   *   . * . . *

                              123               130               140
MDH                           S V E K P V V P V V A I T T T A G T G S E
MgMNO          Kc28                 Q N P P H I A V S T T A G(G)G S E
AmMNO          Kc39           S E N P R N P P H I A V S T T A G T G S E
                              *   .         *   . * . . * * * * . * * *

                                  237   240               250
MDH                               A R E A M A Y A Q Y M A G V A F N N
MgMNO          Kc47               A R E G M X N A Q Y I A G Q A F N S
                                  * * * . *     * * * . * *   * * *

                                                      361
MDH                                                   T Q S N P R
MgMNO          Kc2                                    V E S N P K
AmMNO          Kc4                                   (V)E S N P K
                                                       . * * * .
```

FIG. 5. Alignment of amino acid sequences of N termini and internal peptides of MNOs from *A. methanolica* (AmMNO) and *M. gastri* MB19 (MgMNO) and MDH from the DNA sequence (10) of *B. methanolicus* C1. *, identical residues; ·, conservative substitutions within the series PAGST, QNED, ILVM, HKR, YFW, and C; ?, unidentified residue; -, gap introduced to optimize alignment. Parentheses enclose assignments based on weak evidence.

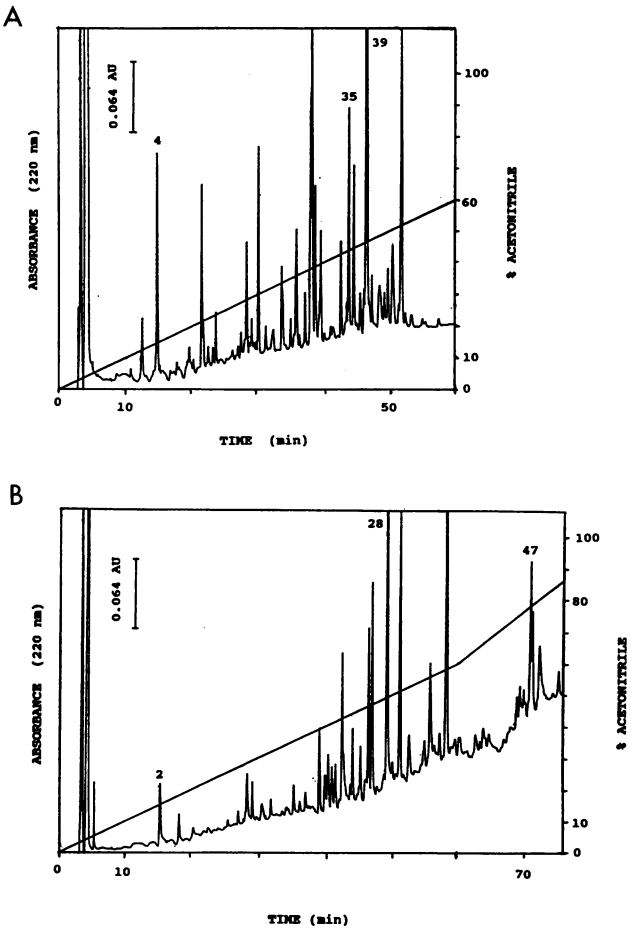

FIG. 6. HPLC separation of Lys-C endoproteinase digests of *A. methanolica* (A) and *M. gastri* MB19 (B) MNOs.

further conservative substitutions have occurred (46% overall similarity). The presence of an 11-amino-acid-residue N-terminal extension in both MNOs (Fig. 5) only partly explains the difference in subunit molecular masses between the MNOs from *A. methanolica* and *M. gastri* (49 to 50 kDa) and *Bacillus* MDH (43 kDa).

The relatedness of the MNOs to *Bacillus* MDH was further studied by sequence analysis of several internal peptides derived by a Lys-C protease digest of the purified MNOs (Fig. 6). Peptides Kc39 and Kc4 from the *A. methanolica* MNO show a high degree of identity with peptides Kc28 and Kc2 from the *M. gastri* enzyme (Fig. 5). Moreover, these four peptides exhibit significant similarity to internal amino acid sequences of *B. methanolicus* C1 MDH, with peptides Kc28 and Kc39 being homologous to a fragment starting at position 123 and peptides Kc2 and Kc4 being homologous to a fragment starting at position 361. In addition, peptide Kc47 of the *M. gastri* enzyme is homologous to an MDH sequence starting at position 237. Thus, in addition to a striking similarity in quaternary protein structures, both MNOs and *Bacillus* MDH possess significant amino acid sequence similarity, suggesting that the three enzymes are evolutionarily closely related.

TABLE 1. Amino acid analysis of *A. methanolica* and *M. gastri* MB19 MNOs

Amino acid	No. of residues (mol/mol subunit)[a]		
	A. methanolica	*M. gastri*	*B. methanolicus*[b]
Glycine	42	49	54
Alanine	42	41	49
Serine	33	33	19
Proline	22	20	14
Valine	31	31	29
Threonine	23	24	20
Isoleucine	20	28	19
Leucine	32	30	22
Aspartic acid	67	56	35
Lysine	33	15	20
Glutamic acid	35	48	36
Methionine	8	9	7
Histidine	14	15	8
Phenylalanine	20	19	10
Arginine	11	15	9
Tyrosine	12	14	8
Total no. of residues	445	447	359

[a] The data presented for the MNO proteins are average values of two separate runs. Tryptophan and cysteine were decomposed during acid hydrolysis.

[b] The amino acid composition of MDH from *B. methanolicus* C1 was calculated from the gene sequence (10), with the amide amino acids being summed up with their corresponding acids.

The MNOs of *A. methanolica* and *M. gastri* show a high degree of similarity with respect to their total amino acid contents (Table 1). The predominant residues in both proteins are Asx, Gly, Ala, Glx, Ser, and Val.

Metal composition. The results of the metal analysis are presented in Table 2. The data indicate that the MNO from *A. methanolica* contains one to two molecules of zinc and magnesium per subunit, a composition which is similar to the metal composition of the NAD-dependent MDH from *B. methanolicus* C1, which contains one zinc and one to two magnesium molecules per subunit (24). The *M. gastri* MNO was also found to possess significant amounts of zinc and magnesium, but in addition, it contained iron. The absolute metal concentrations are much lower, however, than what would be expected if they were stoichiometrically present in the subunits. This is most probably caused by partial dissociation of the metal ions during preparation of the enzyme for metal analysis by dialysis. The exact metal composition of the *M. gastri* enzyme therefore remains unknown.

TABLE 2. Metal contents of purified preparations of MNOs from *A. methanolica* and *M. gastri* MB19

Strain containing MNO	Amt (nmol/ml) of the following compound[a]			
	Subunit	Iron	Zinc	Magnesium
A. methanolica	0.96	0 (0)	1.73 (1.8 ± 0.2)	1.7 (1.8 ± 0.2)
M. gastri	4	1.47 (0.4 ± 0.1)	1.27 (0.3 ± 0.1)	0.37 (0.1 ± 0.1)

[a] The data presented are mean values of two independent analyses. Values in parentheses are metal/subunit ratios.

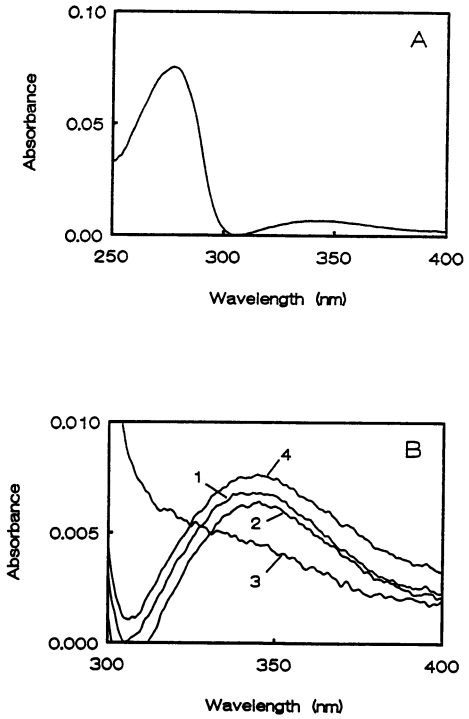

FIG. 7. UV-VIS absorption spectra (A) and UV absorbance spectral analysis (B) of purified MNO from *A. methanolica*. (B) Lines: 1, native spectrum; 2, that plus methanol; 3, that plus acetaldehyde; 4, that plus formaldehyde.

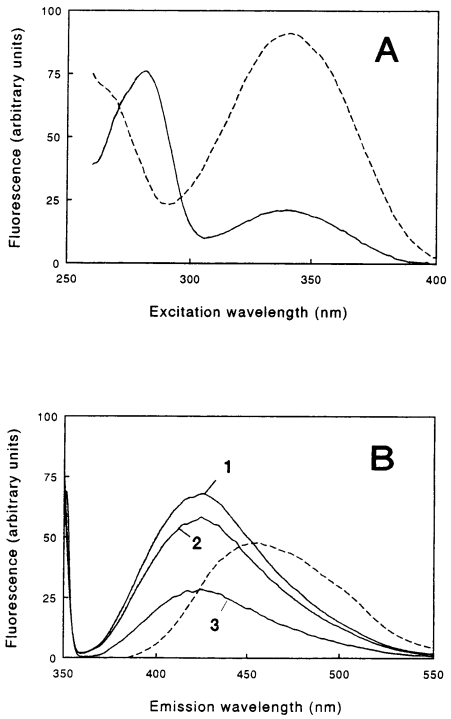

FIG. 8. Fluorescence spectra of purified MNO from *A. methanolica*. (A) Fluorescence excitation spectra at a fixed emission wavelength of 430 nm; (B) fluorescence emission spectra at a fixed excitation wavelength of 340 nm (line 1), with methanol (line 2), and with acetaldehyde (line 3). Broken lines show the spectra of NADPH.

Spectral analysis of the MNO of *A. methanolica*. UV-VIS absorption spectrophotometric analysis of the purified MNO from *A. methanolica* revealed absorption peaks at about 280 and 340 nm (Fig. 7A). Fluorescence excitation spectra (emission at 430 nm) revealed peaks at 285 and 340 nm (Fig. 8A). Both UV-VIS absorbance and fluorescence spectra thus indicated the presence of a chromophore. Fluorescence emission spectra of the enzyme (excitation at 340 nm) showed an emission maximum at 425 nm (Fig. 8B). The emission of the enzyme-bound chromophore decreased slightly when methanol was added. The addition of acetaldehyde caused a significant decrease in emission, whereas formaldehyde had an effect similar to that of methanol. Comparable phenomena were observed with UV absorbance spectral analysis (Fig. 7B). These results show that the MNO-bound chromophore is redox active and most likely is a reduced pyridine nucleotide functioning as a cofactor. The shift in emission optimum of the cofactor compared with that of free NADPH (Fig. 8B) also has been reported for NAD(H)-containing enzymes, e.g., formaldehyde dismutase of *Pseudomonas putida* (18).

Identification and quantification of MNO-bound cofactor. Pyrroloquinoline quinone in the purified MNOs of *A. methanolica* and *M. gastri* could not be demonstrated. HPLC analysis of supernatants of trichloroacetic acid-treated MNOs did not provide evidence for the presence of NAD(P). Ion-exchange chromatography (FPLC) with the urea-treated MNO preparations from both strains, however, yielded material with A_{340} that coeluted with NADPH but not with NADH (Fig. 9). The molar NADPH/subunit ratio was approximately 0.7 for both MNOs. After oxidation by phenazine methosulfate and MTT, the extracted cofactor showed biological activity in an NADP-specific glucose-6-phosphate dehydrogenase assay in which it could replace commercial NADP(H). These data unambiguously show that the purified MNOs of *A. methanolica* and *M. gastri* contain tightly but noncovalently bound NADPH cofactor, most likely at a ratio of one NADP(H) molecule per subunit.

DISCUSSION

In contrast to the well-known enzymology and genetics of methanol oxidation in gram-negative methylotrophs, which involve a periplasmic quinoprotein MDH containing pyrroloquinoline quinone as a prosthetic group (1, 2), little is known about the enzymes of primary methanol oxidation in gram-positive methylotrophs. Only recently, Arfman et al. reported the presence of a cytoplasmic NAD-dependent MDH in thermotolerant *Bacillus* strains, a decameric protein which catalyzes the conversion of methanol to formaldehyde and contains a tightly but noncovalently bound NAD(H) cofactor (4, 5, 24). This raised the question of whether similar enzymes are involved in methanol oxidation in other gram-positive methylotrophs. The results described in this article show that *A. methanolica* and *M. gastri* possess decameric MNOs containing a tightly but noncovalently bound pyridine nucleotide. The cofactor in these enzymes was identified as NADP(H) instead of NAD(H), however. The bound NADP(H) cofactor of *A. methanolica* MNO is redox active toward various alcohol and aldehyde substrates, and therefore, it most likely participates directly in the oxidoreductase and dismutase reactions catalyzed by these enzymes (6).

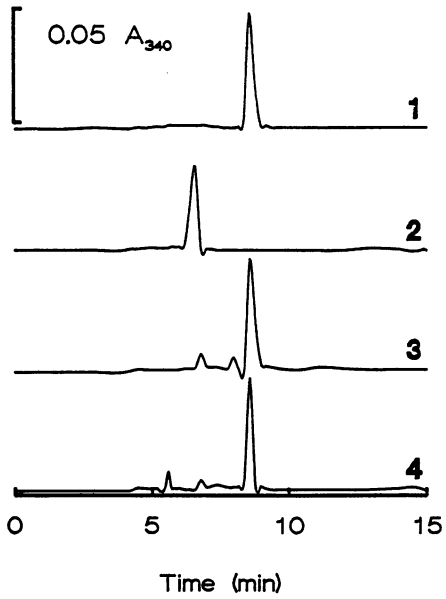

FIG. 9. Ion-exchange chromatographic analysis of authentic NADPH (1), authentic NADH (2), and urea-extracted MNO chromophores of *A. methanolica* (3) and *M. gastri* MB19 (4).

The *A. methanolica* and *M. gastri* MNOs are closely related, as indicated by N-terminal amino acid sequence analysis (63% identity in the first 27 N-terminal amino acid residues), the presence of highly identical internal peptide fragments in both enzymes (Fig. 5), and their similar quaternary structures (Fig. 1). An alignment of the MNO and *Bacillus* MDH amino acid sequences on the basis of the -Gly-X-Gly-17 residues-Leu- sequence pattern, conserved in all type 3 alcohol dehydrogenases (10, 24), revealed considerable similarity and the presence of an 11-amino-acid-residue N-terminal extension in the MNOs. Comparison of internal peptide sequences of the MNOs with the (deduced) amino acid sequence of *Bacillus* MDH, moreover, revealed significant identity with four different internal MDH sequences scattered over the entire enzyme. The data thus indicate that the three enzymes are closely related. Previously, we reported that *B. methanolicus* C1 MDH belongs to a newly established third family of alcohol dehydrogenases (10) distinct from the long-chain horse liver alcohol dehydrogenase type and the short-chain *Drosophila* alcohol dehydrogenase type (16). In addition, the type 3 alcohol dehydrogenases include *Zymomonas mobilis* ADH2 (8), *Saccharomyces cerevisiae* ADH4 (26), *Escherichia coli* 1,2-propanediol oxidoreductase (7), three *Clostridium acetobutylicum* NAD(P)H-dependent butanol dehydrogenases (ADH1, BDH I, and BDH II) (25, 27), and the bifunctional *E. coli* fermentative alcohol dehydrogenase–coenzyme A-linked acetaldehyde dehydrogenase (12). Incorporation of the *A. methanolica* and *M. gastri* MNO enzymes brings the total number of type 3 enzymes to 10. Recently, it was shown that an NAD-dependent alcohol dehydrogenase from *Desulfovibrio gigas* also belongs to type 3 (14).

The subunit molecular masses of the MNOs studied (49 to 50 kDa) are considerably higher than the values for the other type 3 enzymes (about 40 kDa, except for the bifunctional acetaldehyde dehydrogenase enzyme, which consists of 80-kDa subunits). This difference is partly due to an N-terminal amino acid extension in the cases of the *A. methanolica* and *M. gastri* enzymes (Fig. 5). The additional amino acids may be responsible for the strikingly different preferential orientations observed by electron microscopy of *Bacillus* MDH and the two MNOs in this study. However, from the limited number of views that are observed, the three-dimensional structure of the molecules cannot be determined exactly. The very stable preferential orientations of the molecules of all three species and the high level of symmetry make these enzymes good subjects for a three-dimensional reconstruction by the random conical tilt method (19). In this way, the location of the additional mass could be established.

The enzymes responsible for methanol oxidation in methylotrophic microorganisms can be classified into three groups on the basis of the nature of the physiological electron acceptor. Methanol oxidation in eukaryotes (fungi and yeasts) is catalyzed by a peroxisomal flavoenzyme alcohol oxidase (1). In gram-negative methylotrophic bacteria, this reaction is without exception catalyzed by a quinoprotein alcohol dehydrogenase (containing pyrroloquinoline quinone as the prosthetic group) located in the periplasm (1, 2). The situation with gram-positive bacteria, which lack a periplasmic space, is less clear. The only well-studied example is *B. methanolicus* C1, in which the conversion of methanol to formaldehyde is catalyzed by an NAD(H)-containing, NAD-dependent MDH (3, 5, 24). The presence of NAD(P)-containing MNOs in *A. methanolica* and *M. gastri* suggests that a pyridine nucleotide containing alcohol oxidoreductases may be universally involved in methanol oxidation in gram-positive methylotrophic bacteria. All enzymes involved in methanol oxidation studied thus far possess a tightly bound cofactor, suggesting that the presence of a temporary deposit for reduction equivalents is a prerequisite for methanol-converting alcohol oxidoreductases.

Although the methanol-oxidizing enzymes described in this article supposedly function in methanol oxidation in vivo, the identity of the physiological acceptor of the reduction equivalents remains to be elucidated.

ACKNOWLEDGMENTS

We thank Douwe Molenaar and Hans Hektor for their assistance in the fluorescence and UV-VIS absorbance measurements. We thank Wilko Keegstra for help with the image-processing facilities and Klaas Gilissen for printing the electron micrographs.

This work was supported by the Programme Committee for Industrial Biotechnology (The Netherlands), the Netherlands Foundation for Chemical Research (SON), the Netherlands Organization for Scientific Research (NWO), and the Belgian National Incentive Programme on Fundamental Research in Life Sciences initiated by the Science Policy Programming Department (contract BIO/22).

REFERENCES

1. **Anthony, C.** 1982. The biochemistry of methylotrophs. Academic Press, London.
2. **Anthony, C.** 1986. Bacterial oxidation of methane and methanol. Adv. Microb. Physiol. **27**:113–210.
3. **Arfman, N., L. Dijkhuizen, G. Kirchhof, W. Ludwig, K.-H. Schleifer, E. S. Bulygina, K. M. Chumakov, N. I. Govorukhina, Y. A. Trotsenko, D. White, and R. J. Sharp.** 1992. *Bacillus methanolicus* sp. nov., a new species of thermotolerant, methanol-utilizing, endospore-forming bacteria. Int. J. Syst. Bacteriol. **42**:439–445.
4. **Arfman, N., J. Van Beeumen, G. E. de Vries, W. Harder, and L. Dijkhuizen.** 1991. Purification and characterization of an activator protein for methanol dehydrogenase from thermotolerant *Bacillus* spp. J. Biol. Chem. **266**:3955–3960.
5. **Arfman, N., E. M. Watling, W. Clement, R. J. van Oosterwijk,**

G. E. de Vries, W. Harder, M. M. Attwood, and L. Dijkhuizen. 1989. Methanol metabolism in thermotolerant methylotrophic *Bacillus* strains involving a novel NAD-dependent methanol dehydrogenase as a key enzyme. Arch. Microbiol. **152:**280–288.

6. **Bystrykh, L. V., N. I. Govorukhina, P. W. van Ophem, H. J. Hektor, L. Dijkhuizen, and J. A. Duine.** Formaldehyde dismutase and methanol:NDMA oxidoreductase activities in gram-positive bacteria oxidizing methanol. J. Gen. Microbiol., in press.
7. **Conway, T., and L. O. Ingram.** 1989. Similarity of *Escherichia coli* propanediol oxidoreductase (*fucO* product) and an unusual alcohol dehydrogenase from *Zymomonas mobilis* and *Saccharomyces cerevisiae*. J. Bacteriol. **171:**3754–3759.
8. **Conway, T., G. W. Sewell, Y. A. Osman, and L. O. Ingram.** 1987. Cloning and sequencing of the alcohol dehydrogenase II gene from *Zymomonas mobilis*. J. Bacteriol. **169:**2591–2597.
9. **de Boer, L., L. Dijkhuizen, G. Grobben, M. Goodfellow, E. Stackebrandt, J. H. Parlett, D. Whitehead, and D. Witt.** 1990. *Amycolatopsis methanolica* sp. nov., a facultatively methylotrophic actinomycete. Int. J. Syst. Bacteriol. **40:**194–204.
10. **de Vries, G. E., N. Arfman, P. Terpstra, and L. Dijkhuizen.** 1992. Cloning, expression, and sequence analysis of the *Bacillus methanolicus* C1 methanol dehydrogenase gene. J. Bacteriol. **174:**5346–5353.
11. **Frank, J., and M. van Heel.** 1982. Correspondence analysis of aligned images of biological particles. J. Mol. Biol. **161:**134–137.
12. **Goodlove, P. E., P. R. Cunningham, J. Parker, and D. P. Clark.** 1989. Cloning and sequence analysis of the fermentative alcohol-dehydrogenase-encoding gene of *Escherichia coli*. Gene **85:**209–214.
13. **Groen, B. W., M. A. G. van Kleef, and J. A. Duine.** 1986. Quinohemoprotein alcohol dehydrogenase apoenzyme from *Pseudomonas testosteroni*. Biochem. J. **234:**611–615.
14. **Hensgens, C. M. H., J. Vonck, E. F. J. van Bruggen, J. Van Beeumen, and T. A. Hansen.** Purification and properties of an NAD-dependent alcohol dehydrogenase from *Desulfovibrio gigas*, submitted for publication.
15. **Hunkapiller, M. W., and L. E. Hood.** 1983. Analysis of phenylthiohydantoins by ultrasensitive gradient high-performance liquid chromatography. Methods Enzymol. **91:**486–493.
16. **Jörnvall, H., M. Persson, and J. Jeffery.** 1981. Alcohol and polyol dehydrogenases are both divided into two protein types, and structural properties cross-relate the different enzyme activities within each type. Proc. Natl. Acad. Sci. USA **78:**4226–4230.
17. **Kalb, V. F., and R. W. Bernlohr.** 1977. A new spectroscopic assay for protein in cell extracts. Anal. Biochem. **82:**362–371.
18. **Kato, N., T. Yamagami, M. Shimao, and C. Sakazawa.** 1986. Formaldehyde dismutase, a novel NAD-binding oxidoreductase from *Pseudomonas putida* F61. Eur. J. Biochem. **156:**59–64.
19. **Radermacher, M.** 1988. Three-dimensional reconstruction of single particles from random and nonrandom tilt series. J. Electron Microsc. Tech. **9:**359–394.
20. **Van Heel, M.** 1984. Multivariate statistical classification of noisy images (randomly oriented biological macromolecules). Ultramicroscopy **13:**165–184.
21. **Van Heel, M., and J. Frank.** 1981. Use of multivariate statistics in analysing the images of biological macromolecules. Ultramicroscopy **6:**187–194.
22. **Van Heel, M., and W. Keegstra.** 1981. IMAGIC: a fast, flexible and friendly image analysis software system. Ultramicroscopy **7:**113–130.
23. **Van Heel, M., and M. Stöffler-Meilicke.** 1985. Characteristic views of *E. coli* and *B. stearothermophilus* 30S ribosomal subunits in the electron microscope. EMBO J. **4:**2389–2395.
24. **Vonck, J., N. Arfman, G. E. de Vries, J. Van Beeumen, E. F. J. van Bruggen, and L. Dijkhuizen.** 1991. Electron microscopic analysis and biochemical characterization of a novel NAD-dependent methanol dehydrogenase from the thermotolerant methylotrophic *Bacillus* sp. C1. J. Biol. Chem. **266:**3949–3954.
25. **Walter, K. A., G. N. Bennett, and E. T. Papoutsakis.** 1992. Molecular characterization of two *Clostridium acetobutylicum* ATCC 824 butanol dehydrogenase isozyme genes. J. Bacteriol. **174:**7149–7158.
26. **Williamson, V. M., and C. E. Paquin.** 1987. Homology of *Saccharomyces cerevisiae* ADH4 to an iron-activated alcohol dehydrogenase from *Zymomonas mobilis*. Mol. Gen. Genet. **209:**374–381.
27. **Youngleson, J. S., W. A. Jones, D. T. Jones, and D. R. Woods.** 1989. Molecular analysis and nucleotide sequence of the *adh1* gene encoding an NADPH-dependent butanol dehydrogenase in the gram-positive anaerobe *Clostridium acetobutylicum*. Gene **78:**355–364.